Anodic oxidation of sulphite ions on graphite anodes in alkaline solution

J. LU, D.B. DREISINGER and W.C. COOPER
Department of Metals and Materials Engineering, University of British Columbia, Vancouver, BC, Canada, V6T 1Z4

Abstract

The anodic oxidation of sulphite ions in alkaline 1 M Na_2SO_4 solution on graphite rotating disc electrodes has been studied over the range from 25 to 60 °C. The reaction order with respect to sulphite ions is below 1 at low potentials and 1 at high potentials. The reaction order with respect to hydroxide ions is close to zero. Two Tafel slopes were observed, 0.060 V decade^{-1} at low potentials and 0.19–0.20 V decade^{-1} at high potentials. The reaction activation energy was calculated at different potentials. The results obtained, using the potential sweep method, are consistent with those realized using the rotating disc. A possible reaction mechanism has been proposed and the diffusion coefficients of sulphite ions and the diffusion activation energy have been calculated.

List of symbols

a_i	the activity of species i
C	concentration (mol dm^{-3})
C_b	bulk concentration (mol dm^{-3})
C_s	the surface concentration (mol dm^{-3})
D	diffusion coefficient (m^2 s^{-1})
E	electrode potential (V)
E_a	the diffusion activation energy (J mol^{-1})
E°	standard equilibrium potential (V)
E_P	peak potential in linear potential sweep (V)
$E_{P/2}$	potential where $i = i_{p/2}$ in linear potential sweep (V)
F	Faraday constant (96 487 A s mol^{-1})
i	current density (A m^{-2})
i_d	diffusion current density (A m^{-2})
i_k	kinetically controlled current density (A m^{-2})
i_l	limiting current density (A m^{-2})
i_p	peak current density (A m^{-2})
K_1	equilibrium constant between $SO_2(aq)$ and HSO_3^-

K_2	equilibrium constant between HSO_3^- and SO_3^{2-}
k	heterogeneous rate constant (m s^{-1})
m_i	molality of species i (mol kg^{-1})
n	number of electrons transferred
n_r	reaction order
R	gas constant (J K^{-1} mol^{-1})
T	absolute temperature (K)
v	scan rate of potential sweep (V s^{-1})
U^+	the activation energy at the potential = 0 (J mol^{-1})
$U_a^+(E)$	the activation energy at potential (E) (J mol^{-1})

Greek characters

|	
α	charge transfer coefficient
α_a	anodic transfer coefficient
δ_d	the thickness of the diffusion layer (m)
η	overpotential (V)
v	kinematic viscosity (m^2 s^{-1})
ω	angular velocity (s^{-1})

1. Introduction

1.1. *Oxidation of sulphite*

1.1.1. *Background and objective of investigation*
The electrochemical oxidation of sulphite has been studied widely and tried as an anode depolarizer to reduce the overall cell voltage in the production of hydrogen and in copper electrowinning in acid sulphate medium [1–6]. It has also been studied for the removal of SO_2 from waste water [7, 8]. However, there are few reports on the electrochemical oxidation of sulphite in alkaline solutions [9, 10]. There are no reports about the

anodic oxidation of sulphite ions as an alternative anode reaction in alkaline solutions. The objective of this research was to study the anodic oxidation of sulphite in alkaline solutions and in subsequent work to apply the results to the solvent extraction–electrowinning recovery of copper and cyanide from gold mining effluents. The chemistry of the overall process has been discussed by Dreisinger et al. [11]. In summary, copper cyanide is extracted using a guanidine-based extractant, stripped with strong alkaline electrolyte and finally electrolysed in a membrane cell to produce copper metal and a bleed stream for cyanide recovery. The use of a membrane (Nafion®) in the copper electrowinning cell is necessary

to prevent cyanide oxidation at the anode. Unfortunately, the use of a Nafion membrane in the copper electrowinning cell is expensive and it is subject to mechanical damage by the growing metal deposit. Accordingly it was decided to begin to develop a process that did not require the use of the membrane. The possible inclusion of sulphite as a sacrificial species was tested in some proof-of-concept electrowinning experiments and was shown to be promising [12]. With sulphite addition, the cell chemistry would become as follows:

$$Na_2Cu(CN)_3 + \tfrac{1}{2}Na_2SO_3 + NaOH$$
$$\rightarrow Cu + 3NaCN + \tfrac{1}{2}Na_2SO_4 + \tfrac{1}{2}H_2O \qquad (1)$$
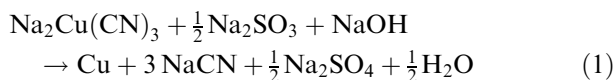
Accordingly, the objective of the present work was to study the anodic oxidation of sulphite ions under alkaline conditions.

1.1.2. *Literature survey*

In neutral and alkaline solutions, the anodic oxidation of sulphite produces sulphate and dithionate and is irreversible [9]. The amount of dithionate produced at the anode surface is a function of the operating conditions, namely anode materials, solution pH and composition, current density [9, 13, 14]. Glasstone and Hickling [13] reported that the optimal pH for the formation of dithionate is in the range 7–9. The sulphite concentration and the temperature have no effect on the dithionate yield. The yield of dithionate on carbon electrodes does not exceed 3% at pH 7.

Conflicting results have been reported on the kinetics and mechanism of the anodic oxidation of sulphite. Klyanina and Shlygin [15] studied the oxidation of sulphur dioxide and sulphite at a platinum electrode and concluded that in acid solutions, only the SO_2 molecule undergoes anodic oxidation at low potentials (0.65–1.2 V vs SHE) by an electron-radical mechanism. The appearance of adsorbed oxygen can completely stop the oxidation by an electron-radical mechanism at potentials > 1.2 V vs SHE. In alkaline solutions, SO_3^{2-} undergoes anodic oxidation beginning at 1.2 V vs SHE. The oxidation mechanism consists of the addition of an OH^- radical to the sulphite ion at relatively high potentials. Tarasevich et al. [10, 16–18] studied the oxidation of sulphite on platinum and carbon electrodes at 22 °C over the pH range 0–14. The reaction order of the electrochemical oxidation depends on the sulphite concentration, being in all cases less than 1. This behaviour may be due to adsorption effects.

In alkaline solutions, sulphite seems to be adsorbed to a lesser extent than in acid solution and the reaction order is close to 1 for up to 0.1 M sulphite. The value of $\partial E/\partial pH$ for the oxidation of sulphite on both pyrographite and activated carbon is close to -40 mV per pH unit in the range of pH 0–7 and becomes zero at higher pH. In alkaline solutions the first Tafel slope is 60–70 mV decade^{-1}. The dependence of the reaction rate on pH is due to variations in the composition of the species which are then subject to oxidation. The adsorbed species undergo deprotonation at pH < 7 and then are subject to oxidation. The slow step involves the transfer of a first or a second electron from the adsorbed species with the formation of the cation radical [10, 16]. The Tafel slope depends on whether the transfer of a first or second electron is the slow step. In alkaline solution, the existence of strongly bound oxygen groups and the lower adsorbability of SO_3^{2-} anions make a direct electron transfer from the SO_3^{2-} species more likely. In this case the slow stage is one without the participation of OH^- ions.

Hunger et al. [7, 8] studied the electrochemical oxidation of sulphite on a graphite anode at pH 9 and 25 °C. They reported that the anodic oxidation of sulphite begins at 0.2 V vs SCE with a poorly defined current density plateau being observed in the range of 0.5–0.7 V vs SCE. Based on the Koutecky–Levich equation, they obtained reaction rate constants, reaction orders of 0.68 and 1.34, and charge transfer coefficients of 0.058 and 0.048, respectively, for natural graphite and graphite impregnated with phenol.

Brevett and Johnson [14] studied the anodic oxidation of sulphite on pure and doped PbO_2 film electrodes at 25 and 65 °C in a $NaHCO_3/Na_2CO_3$ buffer (pH 10). They obtained a reaction order of -0.2 using the same method as Hunger et al. [7, 8]. Stankovic et al. [19] studied the anodic oxidation of sulphite on glassy carbon and reported that the concentration of sulphite ions and temperature greatly influence the reaction rate and the number of transferred electrons for the slow step was close to unity.

The anodic oxidation of sulphite in alkaline solutions has not been investigated thoroughly and the published results are inconsistent. For the purpose of using sulphite oxidation as an alternative anodic reaction in copper cyanide electrowinning, the available information is inadequate and further studies on the anodic oxidation of sulphite in alkaline solution are needed.

1.2. *Formula derivation*

The rotating disc electrode is one of the best tools for studying electrode kinetics and its major advantage lies in the uniform diffusion layer, the thickness of which can be calculated. When the migration of the reactant is negligible, the limiting current density (i_l) equals the diffusion current density (i_d) and can be expressed by the Levich equation:

$$i_l = i_d = 0.62nFD^{2/3}v^{-1/6}\omega^{1/2}C_b \qquad (2)$$

where n is the number of electrons transferred, D the diffusion coefficient, v the kinematic viscosity, ω the rotational speed and C_b the bulk solution concentration. The diffusion coefficients of the sulphite ion can be

calculated from the slopes of the straight lines for the plot of i_l against $\omega^{1/2}$. The current density for mixed kinetics at a rotating disc electrode is determined by the heterogeneous reaction rate and the diffusion of the reactant to the disc surface. The rate of the heterogeneous reaction is equal to the diffusion rate under steady-state conditions. Therefore, when the charge transfer coefficient is independent of the reactant concentration and the reverse reaction is negligible, the current density for a simple redox reaction ($O + ne = R$) can be expressed as [20]

$$i = nFk(C_s)^{n_r} \tag{3}$$

$$i = nFD\left(\frac{dC}{dx}\right)_{surface} = nFD\frac{C_b - C_s}{\delta_d} = i_l\left(1 - \frac{C_s}{C_b}\right) \tag{4}$$

where i is the current density, k the reaction rate constant, C_s the electrode surface concentration, C_b the bulk solution concentration, D the diffusion coefficient, δ_d the diffusion layer thickness and i_l the diffusion limiting current ($nFDC_b/\delta_d$). From Equations 3 and 4, we have the following equations:

$$C_s = C_b\left(1 - \frac{i}{i_l}\right) \tag{5}$$

$$i = nFkC_b^{n_r}\left(1 - \frac{i}{i_l}\right)^{n_r} = i_k\left(1 - \frac{i}{i_l}\right)^{n_r} \tag{6}$$

$$\log i = \log i_k + n_r \log\left(1 - \frac{i}{i_l}\right) \tag{7}$$

where $i_k = nFkC_b^{n_r}$ is the kinetically controlled current. The reaction order can be calculated from the plot of $\log i$ against $\log(1 - i/i_l)$ and the kinetically controlled current can be obtained from the intercept on the ordinate. This method is better than the conventional methods based on two points or the plot of the current density against (rotational speed)$^{1/2}$ which are discussed in monographs by Pleskov and Filinovskii [20] and Opekar and Beran [21]. The reaction order is obtained at constant ionic strength. Furthermore, in this method it is not necessary to know the concentration of the reactant. The exchange current and Tafel slope can be obtained from the plot of i_k against overpotential. If $n_r = 1$ (first order), we can obtain the Koutecky–Levich equation from Equation 6:
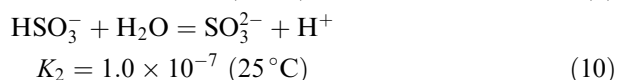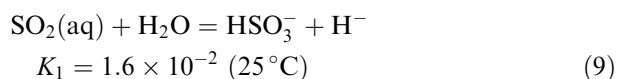
$$\frac{1}{i} = \frac{1}{i_k} + \frac{1}{i_l}. \tag{8}$$

Equations 3, 7 and 8 are also valid for redox reactions such as $O + X + ne = R$ when the reaction order with respect to X is zero or the concentration of X is kept at an elevated level so that there is no difference between the surface and the bulk concentration. In these cases, the kinetic expression can be reduced to Equation 3.

Hunger et al. [7, 8] and Brevett and Johnson [17] calculated i_k using Equation 8 and obtained exchange currents at different sulphite concentrations and, finally, the reaction order of sulphite oxidation using $i_0 = k_0 C_b^{n_r}$. It should be noted that Equation 8 is valid only for a first order reaction.

1.3. Thermodynamics of the anodic oxidation of sulphite

In solution, sulphite exists in the form of SO_2 (aq), HSO_3^- and SO_3^{2-} with the following equilibria between these species [22]:

$$SO_2(aq) + H_2O = HSO_3^- + H^-$$
$$K_1 = 1.6 \times 10^{-2} \ (25\,°C) \tag{9}$$
$$HSO_3^- + H_2O = SO_3^{2-} + H^+$$
$$K_2 = 1.0 \times 10^{-7} \ (25\,°C) \tag{10}$$

SO_2 (aq), HSO_3^- and SO_3^{2-} species are predicted to predominate over the pH ranges <1.8, $1.8–7$ and >7, respectively. At pH >12, the dominant species in solution is SO_3^{2-}. The anodic oxidation of sulphite in alkaline solution on graphite can be expressed by the following equations:

$$SO_3^{2-} + 2\,OH^- = SO_4^{2-} + H_2O + 2\,e^- \tag{11}$$

$$2\,SO_3^{2-} = S_2O_6^{2-} + 2\,e^- \tag{12}$$
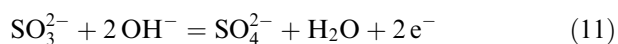
The production of dithionate on graphite (Equation 12) can be neglected according to the literature [13]. The standard equilibrium potentials for Equation 11 are -0.936, -0.957, -0.971, -0.985 V vs SHE at 25, 40, 50 and 60 °C, respectively, obtained by calculation using reliable thermodynamics data [23, 24]. The Nernst equation for the equilibrium potential for Equation 9 is expressed as

$$E = E^\circ + \frac{RT}{2F}\ln\left(\frac{a_{SO_4^{2-}} a_{H_2O}}{a_{SO_3^{2-}} a_{OH^-}^2}\right) \tag{13}$$

The concentration is expressed in molality and so the activity of species i, is $a_i = m_i\gamma_i$. Pitzer's ion–ion interaction model [25, 26] can be used to calculate the activity coefficients of single ion species for multicomponent strong electrolyte solutions and has been used to calculate the activity coefficients of water and hydroxide ions. The interaction of SO_3^{2-} with Na^+ and OH^- is roughly similar to that of SO_4^{2-} [26] and the activity coefficients of SO_3^{2-} and SO_4^{2-} are close [27]. Therefore, the activity coefficient of SO_3^{2-} is assumed to equal to that of SO_4^{2-}.

2. Experimental details

2.1. Equipment and materials

An impregnated NE-150 graphite rod from National Electric Carbon Co. was used to make a graphite

rotating disc. The graphite was machined to 4 mm and tightly surrounded with a plastic shield. The graphite having a 12 mm diameter was fashioned as a rotating disc for the coulometric measurements.

The rotating disc electrode system was an EG&G PARC (model 636) electrode rotator. The potentiostat was a Solartron 1286 electrochemical interface. An EG&G water-jacketed electrolytic cell was used. Argon gas was used to protect sulphite from oxidation by air. A Cannon–Fenske routine viscometer (size 25) was used to measure the kinematic viscosity of the solutions studied.

Reagent grade chemicals were used throughout the investigation.

2.2. Procedure

100 ml of solution of the required composition were added to the electrolytic cell. The experiments were carried out under an argon atmosphere to protect the sulphite from oxidation by air. The ohmic drop between the working electrode and the reference electrode was compensated by the current interruption technique. The electrode surface was first renewed using 600-grit sandpaper, polished with 4000-grit silicon carbide sandpaper and then soft tissue paper. Finally, the surface was checked under a microscope for surface smoothness. To ensure reproducible results, the electrode was first treated by cyclic voltammetry between 0 and 0.75 V vs SCE at $100\,mV\,s^{-1}$ for 30 min and polarized at $1\,mV\,s^{-1}$ until the electrode reached a stable condition. The concentration of sulphite was measured by adding an excess of standard iodine solution followed by back titration with standard thiosulphate solution. The liquid junction potential was calculated by the Henderson equation [28] and the thermal liquid junction potential was measured using two calomel reference electrodes.

3. Results and discussion

3.1. Polarization measurements

The polarization measurements were carried out at 25, 40, 50 and 60 °C in 1 M Na_2SO_4 solution and at concentrations of sulphite in the range 0.025 to 0.5 M. If the applied potential was larger than about 1.0 V vs SCE, the surface of the electrode was corroded and became rough, affecting the current measurements (e.g., the limiting current became much lower and the current against potential was nonreproducible). Therefore, the electrode surface was renewed for every polarization measurement to ensure reproducible results. Typical polarization curves for 0.1 M Na_2SO_3 at 25 and 60 °C are shown in Figure 1. The polarization curves for the other sulphite concentrations were similar. The anodic oxidation of sulphite began at 0.16, 0.12, 0.08 and 0.04 V vs SCE for 25, 40, 50 and 60 °C, respectively. Due to the presence of sulphite ions, oxygen evolution was suppressed and the corrosion of the electrode was
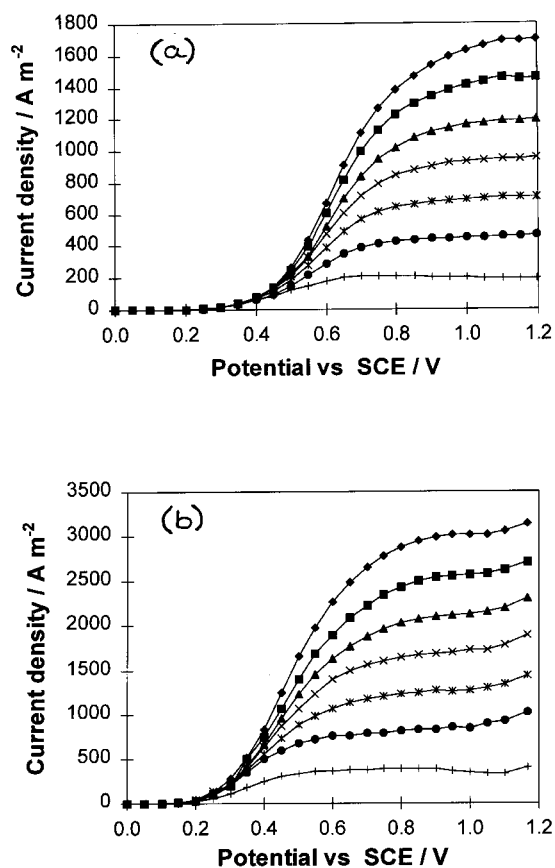

Fig. 1. Polarization curves of sulphite oxidation using a graphite rotating disc at (a) 25 and (b) 60 °C. Electrolyte: 0.1 M Na_2SO_4, 1 M Na_2SO_4 and 0.25 M NaOH. Key: (◆) 4900, (■) 3600, (▲) 2500, (×) 1600, (*) 900, (●) 400 and (+) 100 rpm.

diminished. The higher the concentration of sulphite, the greater were these effects. The limiting current is proportional to the square root of the rotational speed. At a temperature above 50 °C (Figure 1(b)), after the current reached a limiting value and increased further with increasing potential. Gas bubbles formed on the electrode surface due to the evolution of oxygen and possibly the oxidation of graphite. At 100 rpm, the current first decreased a little with increasing potential after the current reached a limiting value because the bubbles formed on the electrode surface were not removed efficiently and the oxygen evolution diminished the oxidation of sulphite. The current finally increased slightly again with increasing potential accompanied by the massive evolution of oxygen. Therefore, the background current in the presence of sulphite could be much smaller than that measured in the absence of sulphite and would make a negligible contribution to the total current. The background current in the absence of sulphite was almost independent of the rotational speed and was not used to correct the current for the sulphite oxidation due to oxygen evolution at high potentials. The condition of the surface of the graphite electrode varied after the electrode surface was renewed each time. Therefore, after the same treatment of the electrode, the values of current against potential scattered to some

extent (±15%). However, the limiting currents scattered less (±2%).

3.2. Coulometric measurements

Controlled potential coulometry was used to determine the number of the electrons transferred (n) for the anodic oxidation of sulphite ion. The electrode potentials were controlled at 0.6 and 0.9 V vs SCE to avoid oxygen evolution and corrosion of the graphite. The results are given in Table 1. In all cases, the number of the electrons transferred per one sulphite ion ranges from 1.92 to 1.98. This means that almost all of the sulphite was oxidized to sulphate in the two-electron reaction. Hence, the oxidation of sulphite to dithionate can be neglected. Potential and temperature had almost no effect on the products of the anodic oxidation of sulphite. These results are in agreement with those reported by Glasstone and Hickling [13].

3.3. Reaction order

For the anodic oxidation of sulphite, the concentrations of sulphite and hydroxide could affect the reaction rate. Therefore the kinetics were first studied by changing the concentration of one species while the potential and the concentrations of the other species were maintained constant. When the potential and pH were maintained constant, the current increased with increasing sulphite concentration, indicating the rate controlling step involved sulphite ions. However, when the potential and sulphite concentration were maintained constant, the current was independent of pH, suggesting that the reaction order with respect to hydroxide is zero. Therefore, only sulphite affects the rate of the sulphite oxidation and the kinetic expression for the anodic oxidation of sulphite ions can be reduced to Equation 3 over the pH range studied. In the mixed control region, Equation 7 can be applied to calculate the reaction order with respect to sulphite. From the plot of $\log i$ against $\log (1 - i/i_l)$, the slope of the line (i.e., the reaction order) and the intercepts on the $\log i$ axis ($\log i_k$) can be calculated.

As has been mentioned, the condition of the surface of the graphite electrode varied after the electrochemical conditioning. The data (current against potential) scattered to some extent due to the inherent surface variability. The data in Figure 1 were generated with different surfaces and therefore cannot be used directly to calculate the reaction order. The data for the reaction order calculation (e.g., Figure 2) were generated on a single stable surface. The stability was maintained by limiting the potential range of the experiments (0–0.7 V vs SCE). A higher potential could change the condition of the electrode surface, making it difficult to obtain reproducible results. From Figure 2, the plot of $\log i$ against $\log(1 - i/i_l)$ at 25 °C is a straight line. The slope of the line (i.e., the reaction order) and the intercepts on the $\log i$ axis ($\log i_k$) were calculated by least squares-fitting and are given in Table 2. The reaction order with respect to sulphite is 1. For the first order reaction, Equation 8 can be applied and the plot of $1/i$ against $1/i_l$ is a straight line and the intercept on the $1/i$ axis is $1/i_k$. From Figure 3, the plots of $1/i$ against $1/i_l$ are linear and the slopes are 1. The intercepts of the plot of $\log i$ against $\log(1 - i/i_l)$ are the same as $-\log$ of the intercepts of the plots of $1/i$ against $1/i_l$ at the same potential (Table 2). This means that the reaction order is 1 and therefore the two methods match very well.

At 40, 50 and 60 °C, the same results were obtained. When the concentration of sulphite was 0.2 M and 0.4 M, the reaction order with respect to sulphite ions was still 1. In the low polarization region, the current is small and therefore the concentrations at the electrode and in the bulk are the same. In this case, only Equation 3 is needed to analyse the kinetics. Equation 7 is not required because the mass transfer is not important. Therefore the reaction order was not calculated using the slope of the plot of $\log i$ against $\log(1 - i/i_l)$, rather it was calculated from the plot of $\log i$ as a function of the sulphite concentration. The plots of $\log(i)$ against $\log[SO_3^{2-}]$ at 0.2 and 0.4 V vs SCE at 25 °C are shown in Figure 4. At 0.4 V vs SCE, the reaction order was 0.95. At 0.2 V vs SCE, the reaction order was below 1 and appeared to be nonlinear with increasing reactant concentration. The reason for this nonlinearity could be caused by the variable adsorption of sulphite ions.

Table 1. Number of the electrons transferred for the anodic oxidation of sulphite

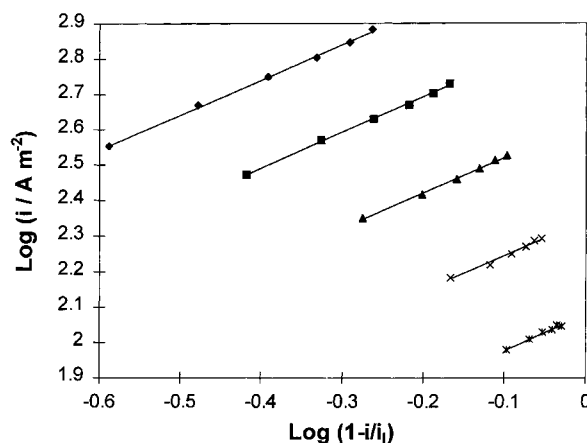| Concentration of sulphite /mol dm^{-3}	Potential vs SCE /V	Temperature /°C	Number of electrons transferred (n) per sulphite ion
0.1	0.6	25	1.94 ± 0.03
0.1	0.9	25	1.98 ± 0.02
0.1	0.6	60	1.93 ± 0.03
0.1	0.9	60	1.97 ± 0.03
0.4	0.6	25	1.92 ± 0.04

Fig. 2. Log i against $\log(1 - i/i_l)$ at constant potential and at 25 °C. Electrolyte: 0.1 M Na$_2$SO$_3$, 1 M Na$_2$SO$_4$ and 0.25 M NaOH. Key: (◆) 0.70, (■) 0.65, (▲) 0.60, (×) 0.55 and (*) 0.50 V vs SCE.

Table 2. Reaction order and the kinetic current calculated using different methods

Potential V vs SCE/V	0.50	0.55	0.60	0.65	0.70
Slope of log i vs log($1 - i/i_l$)	1.05	1.01	1.01	1.01	0.99
Intercepts of log i vs log($1 - i/i_l$) (i.e., i_k/A m^{-2})	2.08	2.35	2.62	2.90	3.14
Slope of plot of $1/i$ vs $1/i_l$	1.04	1.01	1.00	1.01	1.00
$-$Log(intercepts of plot of $1/i$ vs $1/i_l$) (i.e., i_k/A m^{-2})	2.08	2.35	2.62	2.90	3.14
Log($i/(1 - i/i_l)$) (i.e., i_k/A m^{-2})	2.06	2.33	2.61	2.89	3.15

If the reaction order is 1, the plot of $\log(i/(1 - i/i_l))$ (corrected for the difference in concentration of sulphite between the bulk electrolyte and that at the electrode surface) against potential should be a straight line. At low current, $(1 - i/i_l)$ is close to 1 and the concentration difference can be neglected. The plots of $\log(i/(1 - i/i_l))$ against potential at 25, 40, 50 and 60 °C are shown in Figure 5. The corrected current $(i/(1 - i/i_l))$ is the same as the kinetic current (i_k) calculated using the above methods (Table 2).

There are two Tafel slopes. The first Tafel slope at low potentials was 0.059–0.066 V decade^{-1} and the charge transfer coefficient is about 1 and the second Tafel slope at high potentials was 0.19–0.22 V decade^{-1} with the charge transfer coefficient being in the range of 0.29–0.31. The Tafel slopes for the different potentials ranges and temperatures are listed in Table 3. The first Tafel slope (0.060 V decade^{-1}) corresponds to the nonlinear reaction order (less than 1) at low potential (0.16–0.25 V vs SCE) and the second Tafel slope corresponds to the first order region at high potentials (0.4–0.7 V vs SCE) at 25 °C. This information suggests that there are two reaction mechanisms. The change in Tafel slope, hence in the mechanism was not due to the potential-dependent change in the nature of electrode surface because after the electrochemical conditioning, the electrode surface was stable over the potential range 0–0.7 V vs SCE. For example, at 25 °C, the background current was almost constant over the potential range 0–0.6 V vs SCE, but the change in the Tafel slope happened between 0.3–0.4 V vs SCE (Figure 5). The Tafel slope change could be due to: at low potential, the oxidation of the adsorbed sulphite was dominant and at high potential, the oxidation of unadsorbed sulphite was dominant. Tarasevich et al. [10, 18] reported that the first Tafel slope was 0.060–0.070 V decade^{-1} and the reaction order obtained by the change of sulphite concentration was close to 1. These authors did not report a second Tafel slope.
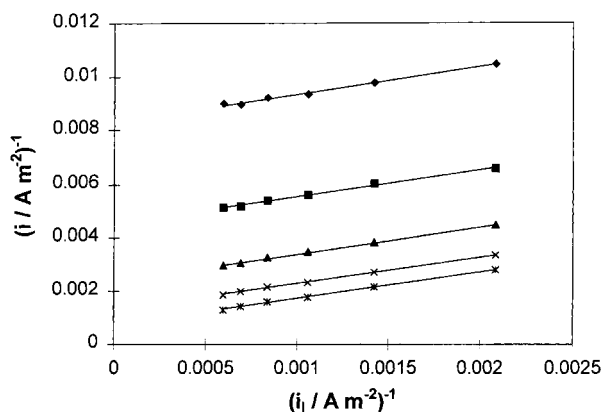
3.4. *Effect of pH*

The effect of pH was studied by changing the sodium hydroxide concentration in the electrolyte containing 1 M Na$_2$SO$_4$. However, the electrolyte contained 1 M Na$_2$SO$_4$ and the pH measurement was not accurate

Fig. 3. $1/i$ against $1/i_l$ at constant potential (V vs SCE) and at 25 °C. Electrolyte: 0.1 M Na$_2$SO$_3$, 1 M Na$_2$SO$_4$ and 0.25 M NaOH. Key: (◆) 0.50, (■) 0.55, (▲) 0.60, (×) 0.65 and (*) 0.70 V.
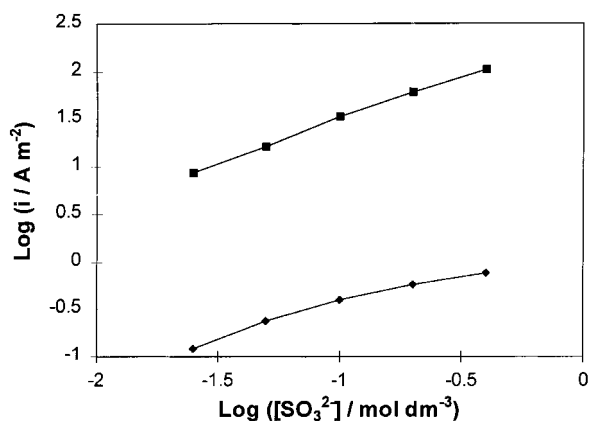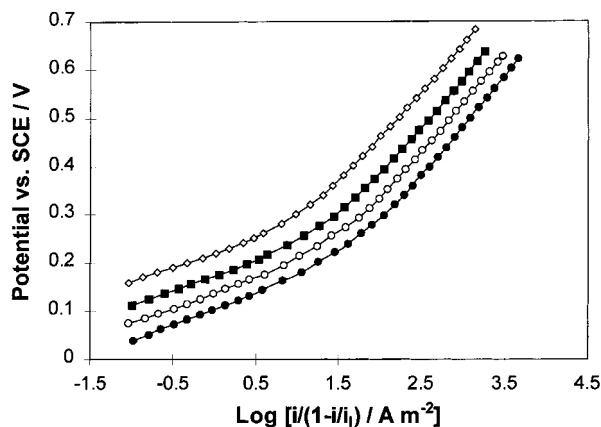

Fig. 4. Log i against log [SO$_3^{2-}$] at 25 °C and 4900 rpm. Electrolyte: 1 M Na$_2$SO$_4$ and 0.25 M NaOH. Key: (◆) 0.2 and (■) 0.4 V vs SCE.

Fig. 5. Potential against log $((i/(1 - i/i_l))$ at different temperatures. Electrolyte: 0.1 M Na$_2$SO$_4$, 1 M Na$_2$SO$_4$ and 0.25 M NaOH. Key: (◇) 25, (■) 40, (○) 50 and (●) 60 °C.

Table 3. Tafel slopes for the different potential ranges at 25, 40, 50 and 60 °C

Temperature	25 °C	40 °C	50 °C	60 °C
Low potential range (V vs SCE)	0.16–0.25	0.11–0.22	0.08–0.18	0.04–0.15
Tafel slopes for low potential range /V decade^{-1}	0.059	0.061	0.064	0.066
High potential range (V vs SCE)	0.4–0.7	0.38–0.66	0.38–0.64	0.36–0.64
Tafel slopes for high potential range /V decade^{-1}	0.19	0.20	0.21	0.22

because the electrolyte had a large background concentration of Na_2SO_4. Therefore, the activity coefficient of OH^- was calculated by Pitzer's model [25, 26]. The value of the activity coefficient of OH^- is 0.48. From Figure 6, the current at a constant potential appears to be almost independent of pH. Therefore the reaction order with respect to OH^- is almost zero. This result is consistent with those reported by Tarasevich et al. [10, 18] and means that the rate-controlling step does not involve OH^-.

3.5. *Calculation of activation energy*

At a constant potential, the following equation can be written:

$$\text{Log } i_k = \text{constant} + \frac{U_a^{\ddagger}(E)}{2.303\,RT}$$
$$= \text{constant} + \frac{U^{\ddagger} - \alpha_a FE}{2.303\,RT} \qquad (14)$$

Where $U_a^{\ddagger}(E)$ is the activation energy at potential E, $U^{\ddagger}$ the activation energy at potential $= 0$, α_a the anodic charge transfer coefficient and R the gas constant. The activation energy can be calculated from the slope of the plot of log i_k against $1/T$ (Figure 7). The slopes of these linear plots were calculated by least-squares fitting. The activation energy decreases quickly with increasing potential at low potentials and finally behaves linearly with potential at potentials >0.4 V vs SCE. This is due to a change in the reaction mechanism which results in a change in the charge transfer coefficient.
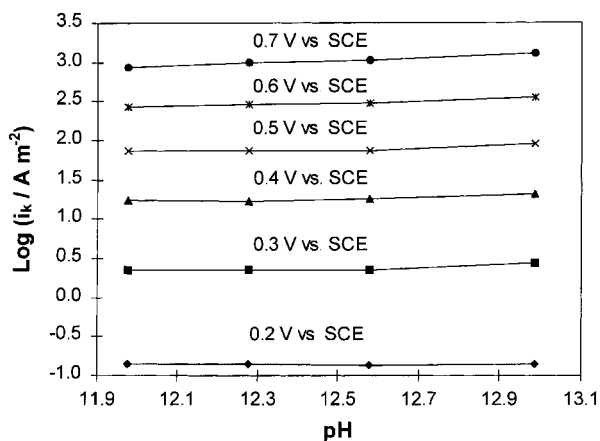
3.6. *Diffusion coefficient estimation*

The plots of diffusion current against rotational speed at different temperatures are shown in Figure 8. These plots permit the calculation of the diffusion coefficients using the slopes of the lines and Equation 2. The slopes were calculated using least-squares fitting. The diffusion coefficients at 25, 40, 50 and 60 °C are 5.6, 8.6, 9.99 and $12.4 \times 10^{-10}\,m^2\,s^{-1}$, respectively. The diffusion coefficient obtained at 25 °C ($5.6 \times 10^{-10}\,m^2\,s^{-1}$) is much lower than the value at infinite dilution ($1.06 \times 10^{-9}\,m^2\,s^{-1}$) [29]. This difference could be caused by the high ionic strength (above 3.1 M) where the ion–ion interaction is significant and the kinematic viscosity is 35% greater than that for water, decreasing the diffusion coefficient. The diffusion coefficient at 25 °C is close to the values ($6–7 \times 10^{-10}\,m^2\,s^{-1}$ in 0.5 M Na_2SO_4) reported by Hunger et al. [7]. The diffusion coefficient has the following temperature dependence:

$$\text{Log } D = \text{constant} - \frac{E_a}{2.303\,RT} \qquad (15)$$

where D is the diffusion coefficient, E_a the diffusion activation energy, R the gas constant, T the absolute temperature.

The diffusion activation energy calculated from the slope of the log plot of diffusion coefficient against $1/T$ (Figure 9) is $18\,kJ\,mol^{-1}$.

3.7. *Potential sweep study*

The potential sweep method was used to study the anodic oxidation of sulphite. Figure 10 shows the cyclic

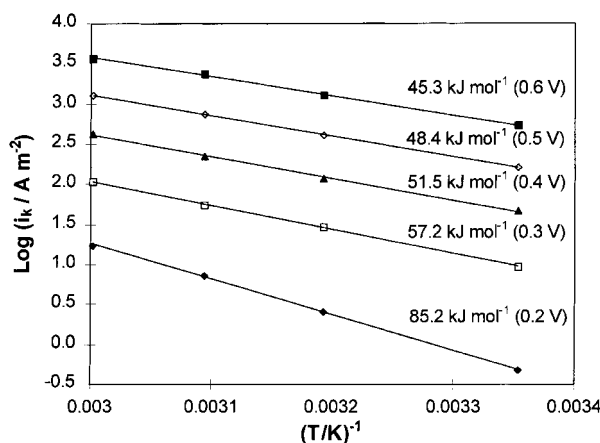*Fig. 6.* Effect of pH on sulphite oxidation at different potentials and at 25 °C. Electrolyte: 0.1 M Na_2SO_3, 1 M Na_2SO_4 at variable pH (calculated using Pitzer's model).

Fig. 7. Log i_k against $1/T$ at different potentials (V vs SCE). Electrolyte: 0.1 M Na_2SO_3, 1 M Na_2SO_4 and 0.25 M NaOH.
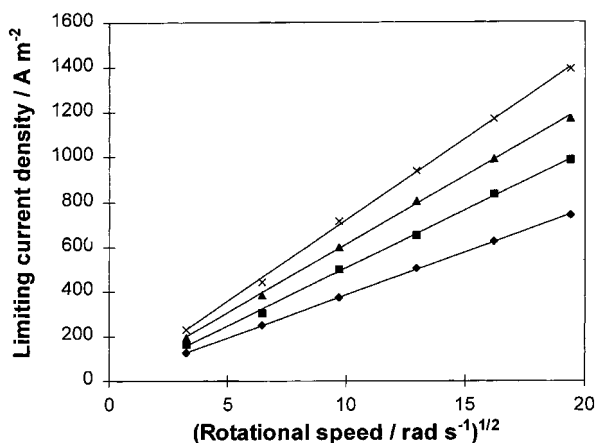
Fig. 8. Diffusion current density against (rotational speed)$^{1/2}$ at different temperatures. Electrolyte: 0.05 M Na$_2$SO$_3$, 1 M Na$_2$SO$_4$, 0.25 M NaOH. Key: ($\blacklozenge$) 25, ($\blacksquare$) 40, ($\blacktriangle$) 50 and ($\times$) 60 °C.

voltammograms after subtraction of the background current for different scan rates. There is no negative current corresponding to the reduction of the oxidized products (or intermediates) and the oxidation of sulphite is irreversible. The peak current density (i_p) is given by the following equation for the irreversible reaction [30]:

$$i_p = (2.99 \times 10^5)n(\alpha)^{1/2}C_bD^{1/2}v^{1/2} = Bv^{1/2} \quad (16)$$

where n is the number of transferred electrons, α the rate-controlling step charge transfer coefficient, C_b the bulk reactant concentration, D the diffusion coefficient, v the potential scan rate and $B = (2.99 \times 10^5) \times n(\alpha)^{1/2}C_bD^{1/2}$. The peak current is proportional to the square root of the potential scan rate. The plot of i_p against $v^{1/2}$ gave a linear relationship (Figure 11). The slope (B) was calculated by least-squares fitting. The following relationship obtains:

$$|E_p - E_{p/2}| = \frac{1.875\,RT}{\alpha F} \quad (17)$$

where E_p is the peak potential and $E_{p/2}$ the potential when $i = i_p/2$.
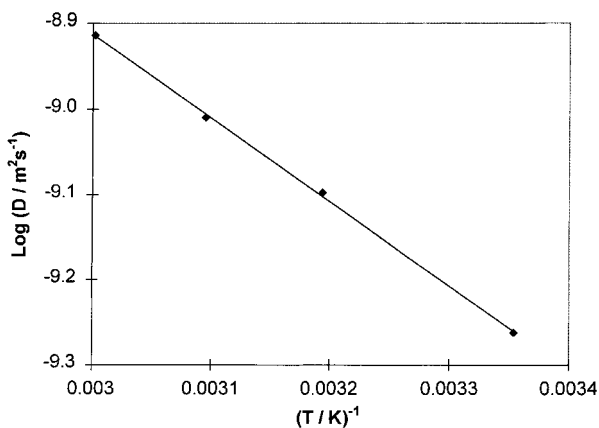

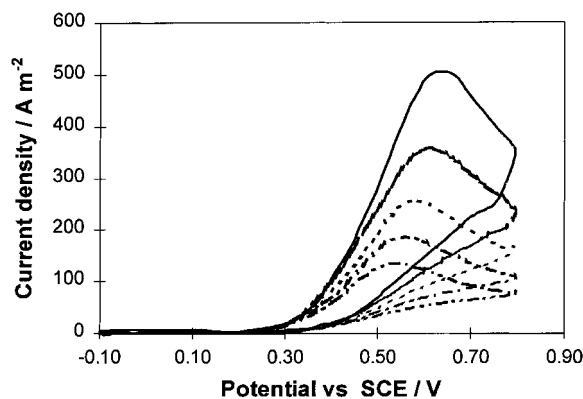Fig. 9. Log plot of diffusion coefficient against $1/T$.

Fig. 10. Voltammograms at different scan rates at 25 °C. Electrolyte: 0.1 M Na$_2$SO$_3$, 1 M Na$_2$SO$_4$, 0.25 M NaOH. Key: (—) 320, (– –) 160, (- - - -) 80, (– - –) 40 and (– - -) 20 (mV)$^{-1}$.

From the above equation we obtain an apparent charge transfer coefficient of 0.33 which is close to that (0.30–0.31) calculated using the Tafel slope at high potentials. The total number of the electrons transferred is 1.98, 1.98, 2.00, 1.98 by combination of B, C_b, α_a, D at 25, 40, 50 and 60 °C, respectively. This number corresponds to the stoichiometry indicated by Equation 11.

From Figure 11 there were no prewaves or postwaves for the positive-going sweep, meaning the reactant and products did not adsorb or adsorbed only weakly on the electrode surface.

3.8. Possible reaction mechanism

From Figure 5, there are two Tafel regions. The first one is 0.059–0.066 V decade^{-1} from 25 to 60 °C at low potentials and the second is 0.19–0.22 V decade^{-1} at higher potentials. The corresponding charge transfer coefficients are 1 and 0.3, respectively. These values suggest a change in the reaction mechanism or in the rate-controlling step. The reaction order at low potentials is below 1 and nonlinear, and decreases slightly with increasing sulphite concentration indicating that the adsorbed sulphite could begin to be oxidized at low potentials. There are no peaks corresponding to the
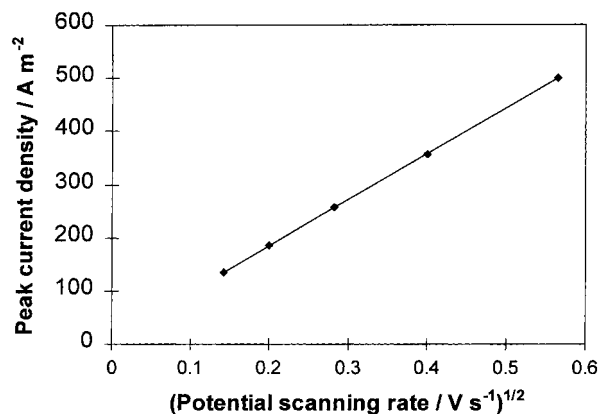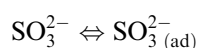

Fig. 11. Peak current against the potential scan rate at 25 °C. Electrolyte: 0.1 M Na$_2$SO$_3$, 1 M Na$_2$SO$_4$ and 0.25 M NaOH.
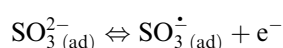
adsorption in the voltammograms. This means that sulphite adsorbs weakly on the electrode surface. Tarasevich et al. [17] studied the adsorption and electrooxidation of sulphite on platinum using radioactive tracers and found that SO_3^{2-} was weakly adsorbed on the surface and the amount of adsorbed SO_3^{2-} did not change over the potential range -0.24–0.26 V vs SCE and decreased to zero with increasing potential from 0.26 to 0.56 V vs SCE at 22 °C. In this study, SO_3^{2-} begins to be oxidized on a graphite anode at 0.16 V vs SCE at 25 °C and the Tafel slope was maintained at a constant value of 0.060 V decade^{-1} over the potential range 0.16–0.25 V vs SCE. With further increase in potential, the Tafel slope increased with increasing potential and when the potential exceeded 0.4 V vs SCE, the Tafel slope remained at 0.19 V decade^{-1} and was independent of the potential. The above phenomenon can be explained by: (i) at 0.16–0.25 V vs SCE, the adsorbed SO_3^{2-} is oxidized and the coverage of adsorbed SO_3^{2-} was independent of potential and therefore the Tafel slope (0.060 V decade^{-1}) is independent of the potential and the reaction order with respect to SO_3^{2-} was below 1 and nonlinear; (ii) at 0.25–0.4 V vs SCE, the coverage of adsorbed SO_3^{2-} decreases with increasing potential. Therefore, the Tafel slope increased with increasing potential; (iii) at potential >0.4 V, the amount of adsorbed SO_3^{2-} is negligible and the direct oxidation of unadsorbed SO_3^{2-} dominates. Thus the Tafel slope became independent of the potential and the reaction order with respect to SO_3^{2-} became unity. The reaction order with respect to OH$^-$ ions is almost zero. This means that the rate-controlling steps for the two Tafel slope regions do not involve OH$^-$. There are numerous carbon oxide surface groups on graphite [10, 31] and sulphur could be bound to these surface groups during the adsorption. In accordance with the these phenomena, the following reaction mechanism is proposed.

At low potentials (<0.25 V vs SCE), sulphite first adsorbs on the graphite, then loses the first electron, and finally undergoes oxygen transfer and loses the second electron. For example,
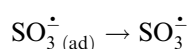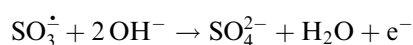
Step 1

$$SO_3^{2-} \Leftrightarrow SO_{3\ (ad)}^{2-}$$

Step 2

$$SO_{3\ (ad)}^{2-} \Leftrightarrow SO_{3\ (ad)}^{\cdot -} + e^-$$

Step 3

$$SO_{3\ (ad)}^{\cdot -} \rightarrow SO_3^{\cdot -}$$

Step 4

$$SO_3^{\cdot -} + 2\,OH^- \rightarrow SO_4^{2-} + H_2O + e^-$$

Considering the theory of multistep electrode reactions [32, 33], if step 1 is the rate-controlling step, the current

should be independent of potential. If step 2 is the rate-controlling step, the Tafel slope should be around 0.12 V decade^{-1}. If step 4 is the rate-controlling step, the Tafel slope should be around 0.040 V decade^{-1} and the reaction order with respect to OH$^-$ ions should be 1 or more. If step 3 is the rate-controlling step, the Tafel slope is 0.060 V decade^{-1}. The reaction order with respect to OH$^-$ ions could be zero. Looking at the experimental results, step 3 could be the rate-controlling step. In addition, step 4 could consist of several steps.

At high potentials (>0.4 V vs SCE), sulphite first loses one electron, subsequently undergoes oxygen transfer and loses the second electron.

Step 1

$$SO_3^{2-} \rightarrow SO_3^{\cdot -} + e^-$$

Step 2

$$SO_3^{\cdot -} + 2\,OH^- \rightarrow SO_4^{2-} + H_2O + e^-$$
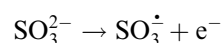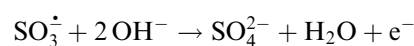
The charge transfer coefficient is only about 0.3, suggesting that the loss of the first electron is the rate-controlling step. This is in agreement with the reaction order with respect to sulphite ions. The reaction order with respect to hydroxide ions is zero, suggesting that the rate-controlling step does not involve hydroxide ions. Therefore, step 1 could be the rate-controlling step at high potentials. It should be noted that a small amount of $SO_3^{\cdot -}$ could combine to form dithionate and therefore the number of the electrons transferred is slightly below 2.

4. Conclusions

(i) A modified rotating disc electrode method can be used to calculate the reaction order and the kinetic current for the oxidation of sulphite ions.

(ii) At low potentials (e.g., <0.25 V vs SCE at 25 °C), the reaction order for the oxidation of sulphite is below 1 and decreases with increasing concentration. The Tafel slope is 0.060–0.065 V decacde^{-1}. At high potentials (>0.4 V vs SCE), the reaction order with respect to sulphite ions is 1 up to 0.4 M and the Tafel slope is 0.19–0.21 V decade^{-1}.

(iii) The reaction order with respect to hydroxide ions is close to zero.

(iv) The diffusion coefficients of sulphite ions were obtained and shown to have an activation energy of 18 kJ mol^{-1}.

(v) Sulphite oxidation in alkaline solution appears to undergo a radical-electron mechanism. At low potentials, the adsorbed sulphite oxidation is dominant and at high potentials, the sulphite ions are oxidized directly on the electrode surface. The loss of the first electron from sulphite ions appears to be the rate-controlling step at high potentials.

1170

References

1. G.F. Pace and J.C. Stauter, *CIM Bulletin* (1974) 85.
2. A.V. Cooke, J.P. Chilton and D.J. Fray, 'Anode Depolarisers in the Electrowinning of Copper', Extraction'81, The Institute of Mining and Metallurgy, London, England (1981), pp. 430–441.
3. K.K. Mishra and W.C. Cooper, 'Electrochemical Aspects of the Direct Electrowinning of Copper from Sulphuric Acid Leach Solutions in the Presence of Iron Using Gas Sparging', Anodes for Electrowinning, Proceedings of the Metallurgical Society, AIME Annual Meeting, Los Angeles, CA (1984), pp. 13–26.
4. D.J. Robinson, *J. Met.* (1984) 43.
5. K.A. Spring and J.W. Evans, *J. Appl. Electrochem.* **15** (1985) 609.
6. A.J. Appleby and B. Pichon, 'Electrochemical Aspects of the H_2SO_4–SO_2 Thermoelectrochemical Cycle for Hydrogen Production', Proceedings of the 2nd World Hydrogen Energy Conference, Zurich, Switzerland, 21–24 Aug., (1978), pp. 687–797.
7. T. Hunger, F. Lapicque and A. Storck, *J. Appl. Electrochem.* **21** (1991) 588.
8. T. Hunger and F. Lapicque, *Electrochim. Acta* **36** (1991) 1073.
9. S.I. Zhdanov, *in* 'Encyclopedia of the Electrochemistry of the Elements' (edited by A.J. Bard), Vol. 4 (Marcel Dekker, New York, 1975), pp. 330–335.
10. M.R. Tarasevich and E. I. Khrushcheva, *in* 'Modern Aspects of Electrochemistry', No. 19 (edited by B.E. Conway, J.O'M Bockris and R.E. White), (Plenum Press, 1989), pp. 295–359.
11. D.B. Dreisinger, J. Ji and B. Wassink, 'The Solvent Extraction–Electrowinning of Copper and Cyanide Using XI 7950 Extractant and Membrane Cell Electrolysis: Benchscale and Mini-Pilot Plant Studies', Proc. Randol Gold Forum, Perth (1995), pp. 239–244.
12. D.B. Dreisinger and J. Lu, unpublished results (1997).
13. S. Glasstone and A. Hickling, *J. Chem. Soc.* (1933) 829.
14. C.A.S. Brevett and D.C. Johnson, *J. Electrochem. Soc.* **139** (1992) 1314.
15. G.L. Klyanina and A.I. Shlygin, Russian *J. Phys. Chem.* **36** (1962) 692.
16. K.A. Radyushkina, M.R. Tarasevich, O.A. Levina and V.N. Andreev, *Electrokhimiya* **18** (1982) 1166.
17. M.R. Tarasevich, V.N. Andreev, V.E. Kazarinov, O.A. Levina and K.A. Radyushkina, *Electrokhimiya* **18** (1982) 1402.
18. N.A. Urisson, G.V. Shteinberg, M.R. Tarasevich, and V.S. Bagotskii, *Electrokhimiya* **19** (1983) 243.
19. V.D. Stankovic, Z.D. Stankovic and M. Rajcic-Vujasinovic, 'Electrochemical Oxidation of Sulphite Ions', ISE 46th Annual Meeting (1995), Vol. 2, p. 8–05.
20. Yu.V. Pleskov and V.Yu. Filinovskii, 'The Rotating Disc Electrode' (translated by Halina S. Wroblowa, edited by Halina S. Wroblowa and B. E. Conway), Consultants Bureau, New York (1976).
21. F. Opekar and P. Beran, *J. Electroanal. Chem.* **69** (1976) 1.
22. N.N. Greenwood and A. Earnshaw, 'Chemistry of the Elements' (Pergamon Press, New York, 1990), Chapter 15, pp. 851–853.
23. A.J. Bard, R. Parsons and J. Jordan, 'Standard Potentials in Aqueous Solution', IUPC (1985), pp. 93–125.
24. G. Milazzo, S. Caroli, and V.K. Sharma, 'Tables of Standard Electrode Potentials', Project of the IUPAC Electrochemistry Commission (J. Wiley & Sons, New York, 1978), p. 239.
25. K.S. Pitzer and J.J. Kim, *J. Am. Chem. Soc.* **96** (1974) 5701.
26. K.S. Pitzer, 'Activity Coefficients in Electrolyte Solution', 2nd edn, CRC Press, Boca Raton, FA (1991), chapters 3 and 6.
27. J. Kielland, *J. Am. Chem. Soc.* **59** (1937) 1675.
28. P. Henderson, *Z. Physik. Chem.* **59** (1907) 118, *ibid.* **63** (1908) 325.
29. D.R. Lide and H.V. Kehiaian, 'CRC Handbook of Thermophysical and Thermochemical Data' (CRC Press, Boca Raton, FA, 1994), p. 427.
30. A.J. Bard and L.R. Faulkner, 'Electrochemical Methods – Fundamentals and Applications' (J. Wiley & Sons, New York, 1980), chapter 6, pp. 213–248.
31. K. Kinoshita, *in* 'Carbon – Electrochemical and Physicochemical Properties' (J. Wiley & Sons, New York, 1988), pp. 86–173.
32. J.O'M. Bockris, 'Modern Aspects of Electrochemistry, No. 1', (edited by J.O'M. Bockris and B.E. Conway), (Butterworths, London, 1954), Chapter 4.
33. J.O'M. Bockris and A.K.N. Reddy, 'Modern Electrochemistry', Vol. 2 (Plenum Press, New York, 1970), Chapter 9.